Electronic Supplementary Material (ESI) for Nanoscale. This journal is © The Royal Society of Chemistry 2019

Supporting Information

From fiber curls to mesh waves: A platform for fabrication of hierarchically structured nanofibers mimicking natural tissue formation

*Honglin Chen, Danielle F. Baptista, Giuseppe Criscenti, João Crispim, Hugo Fernandes, Clemens van Blitterswijk, Roman Truckenmüller*and Lorenzo Moroni**

Experimental

Depositing fibers on monoaxially oriented PLA shrink films: PolyActive PEOT/PBT block copolymers having a PEOT/PBT weight ratio of 55/45, the starting poly (ethylene glycol) segments had a molecular weight of 300Da, were obtained from PolyVation (Groningen, The Netherlands). The polymer solution for electrospinning was prepared by dissolving PEOT/PBT in chloroform/1,1,1,3,3,3-hexafluoro-2-propanol (HFIP) (v/v = 4:1) with a final concentration of 20% (w/v) and stirred overnight at room temperature for complete dissolution. The solution was then loaded into a 5 mL syringe attached to a needle with an inner diameter of 0.8 mm and controlled by a syringe pump. The flow rate was adjusted to 0.5 mL/h. A high voltage of 16 kV was applied, and the distance of tip-to-collector was set to 15 cm. The temperature and relative humidity of the electrospinning chamber, which were kept the same for all electrospinning experiments, were controlled at 25 °C and 30%, respectively. Fibers were deposited on oriented PLA films (4 cm x 4 cm) which were placed on a conducting collector plate (for random deposition) or two electrodes (for aligned deposition). In case of collecting aligned fibers, changing the orientation of the PLA film relative to the electrodes for the duration of spinning allows for deposition of fibers according to different orientations: parallel, diagonal and perpendicular orientations relative to the direction of stretching and shrinkage were used in this experiment. The fiber density was adjusted by controlling the deposition time. To investigate the influence of deposition orientation on curling of fibers deposited in a low density, fibers were collected for 2 s on each PLA film. To investigate the effect of (higher) fiber density on curled patterns, fibers were collected up to 45 min.

Fiber-film constructs were then kept in an oven, pre-heated to 75 ± 1 °C, for 1 min to allow shrinkage of the PLA films or film frames, and formation of the buckled fibers or fiber meshes.

Tailoring buckled patterns by selective sacrificial fibers: PVA was dissolved in ethanol/water (v/v = 1:4) at a final concentration of 8% (w/v) while the recipe for PEOT/PBT solution was the same as described above. To investigate low fiber densities, PEOT/PBT and PVA aligned fibers were deposited on PLA films sequentially in a layer-by-layer way. The tip-to-collector distance and voltage applied, which were kept the same for the PEOT/PBT and the PVA solutions, were set to 15 cm and 16 kV, respectively. The feeding rates of the PEOT/PBT and the PVA solutions were adjusted to 0.5 mL/h and 2 mL/h, respectively. To investigate the effect of sacrificial fibers on fiber meshes, PEOT/PBT and PVA fibers were electrospun simultaneously from two corresponding syringes and collected by a mandrel with a rotating speed of 350 rpm around which a PLA film was wound. The two syringes were set up on sides of the mandrel with a 90-degree angle. Both tip-to-collector distances were 12 cm. The feeding rates for PEOT/PBT and PVA were 5 mL/h and 1 mL/h, respectively. The same voltage of 16 kV was applied for both solutions.

Fiber-film constructs were then transferred to an oven, pre-heated to 75 °C ± 1 °C, for 1 min to allow shrinking of the PLA films and formation of the buckled fibers or fiber meshes. Finally, the fiber-film constructs were immersed in water for 30 min to remove the PVA fibers.

Tailoring curled features via varying shrinkage percentage of thermo-shrinkable materials: PEOT/PBT fibers were deposited on oriented PLA films which were placed on the top of a static collector. There, the fibers were collected for 30 min. To investigate the influence of the shrinkage percentages of the films on the curly patterns, the fiber-film constructs were shrunk at 65 °C for different time periods.

Influence of shape and geometry of thermo-shrinkable materials on curled features: To fabricate a fiber mesh with a multiscale crimped pattern, a frame punched out from a PLA film was put on the top of a pair of electrodes to collect the fibers. The spinning parameters for the PEOT/PBT fibers were the same as described above. The fibers were collected for 1 min. To obtain a tubular curled scaffold, PEOT/PBT fibers were collected for 30 min using a mandrel wrapped with an oriented PLA film stripe and rotating with a speed of 150 rpm. The feeding rate of the polymer solution was 5 mL/h. The distance between the needle tip and the collector was set to 12 cm and the applied voltage was 16 kV.

Fiber-film constructs were then transferred to an oven, pre-heated to 75 °C ± 1 °C, for 1 min to allow shrinking of the PLA film tube and formation of a buckled fiber mesh.

Buckled PVA, PAN and PS fibers using PLA films: PVA was dissolved in ethanol/water (1:4) at a concentration of 8% (w/v) and stirred overnight before electrospinning. The applied voltage was 16 kV, the distance between needle tip and collector was 15 cm and the feeding rate of the polymer solution was 1 mL/h. Aligned fibers were collected using a pair of electrodes over which the PLA films were placed. For electrospinning of PAN fibers, 10% polymer solution was prepared by dissolving PAN (MW = 150,000; Sigma) in dimethylformamide (DMF) and stirring the solution overnight at 60 °C to dissolve the polymer completely. The optimized feeding rate of the polymer, applied voltage and tip-to-collector distance was 1 mL/h, 16 kV and 15 cm, respectively. Aligned fibers were collected using a pair of electrodes with the PLA films on top of it. The fibers were collected for between 10 s and 5 min. PS (MW = 350,000; Sigma) was dissolved in DMF at room temperature under stirring overnight to obtain a 20% (w/w) homogeneous solution. The polymer solution was delivered at a rate of 0.5 mL/h. Electrospinning was carried out at 18 kV and 15 cm distance from tip to collector. Aligned fibers were deposited on the PLA films which were placed on top of a pair of electrodes.

Fiber-film constructs were then transferred to an oven, pre-heated to 75 ± 1 °C, for 1 min to allow shrinkage of PLA films and formation of buckled fiber meshes.

Buckled PEOT/PBT and PAN fibers using shrinkable PS materials: The electrospinning process for PEOT/PBT fibers was the same as described above except for the fiber collection. For collecting random fibers, a biaxially oriented thermo-shrinkable PS film with a maximum shrinkage percentage of around 50% was put on top of a static plate collector. For collecting aligned fibers, the PS film was wrapped around a mandrel with a high speed of 5000 rpm. The thickness of the fiber meshes was controlled by the deposition time. The fabrication of PAN fibers was also the same as described above. PAN fibers were deposited on biaxially oriented thermo-shrinkable PS films placed on top of a pair of electrodes. The fibers were collected for 10 s. For both PEOT/PBT and PAN fibers, their fiber-film constructs were then transferred to an oven, pre-heated to 120 °C, for 15 min to allow shrinkage of the PS film and formation of buckled fiber materials.

Characterization of buckled fibers: To check the morphology of scaffolds, samples were sputter-coated with gold and then observed under a SEM (Philips XL-30) at an accelerating voltage of 10 kV. For the low-density meshes, the wavelength and amplitude were measured using Image J; 40 fibers were measured for each condition (5 images with 8 fibers each). The wavelength of curly features was considered as the distance between two consecutive peaks; the amplitude was measured as the distance between the maximum and minimum deflection of the wave divided by two.

Uniaxial tensile tests were performed to evaluate the mechanical properties of different curled structures. Six different percentages of shrinkage (10, 25, 30, 40 and 50%), obtained by varying the exposition time to the shrinkage temperature, were analyzed while non-curly fibers were used as control. A total of 7 samples for each type was tested. The samples were given a rectangular shape using a surgical scalpel so that the length-to-width aspect ratio (4:1; 40 mm/10 mm) ensured uniform tensile stress in the region where the strain was measured. All samples had a similar initial cross-sectional area (CSA) after shrinking and before tensile testing and an average thickness of 642 μm before tensile testing, which was measured with a digital calliper (accuracy of 0.02 mm and resolution of 0.01 mm), and we assumed it had a rectangular shape. The samples were fixed in standard clamps and axially aligned to the 500 N load cell of a Zwick Z020 material testing machine. The scaffolds were preconditioned by a series of 10 cycles where they were exposed up to 3% of strain at a strain rate of 0.1%/s, in order to reduce hysteresis. The samples were then pulled until failure at a strain rate of 0.3%/s. With initial CSA values and strain measurements, a stress-strain curve representing the tensile mechanical properties of the different scaffolds was plotted. From the stress-strain curves, the following parameters were obtained: Young's Modulus

(Pa), defined as the slope of the linear region of the stress-strain curve, ultimate stress (Pa), ultimate strain (%) and strain energy density (Pa). The failure modes were also noted.

hMSC culture and seeding: Pre-selected hMSCs (donor No. 8001L) were obtained from the Institute of Regenerative Medicine at Texas A&M University. Briefly, a bone marrow aspirate was drawn and mononuclear cells were separated using density centrifugation. The cells were plated to obtain adherent hMSCs, which were harvested when cells reached 60–80% confluence. These were considered passage zero (P0) cells. The P0 cells were expanded, harvested and frozen at passage 1 (P1) for distribution. hMSCs were thawed and expanded in T-flasks till reaching 80% confluence in basic medium composed of α Minimum Essential Medium (α-MEM; Gibco), 10% FBS (Lonza), 2 mM L-glutamine (Gibco), 0.2 mM ascorbic acid (Sigma), 100 U/mL penicillin and 100 mg/mL streptomycin (Gibco).

Electrospun samples were punched to fit 48-well plates. After sterilization with 70% ethanol for 2 × 15 min each, the samples were washed with phosphate-buffered saline (PBS) 3 times, and then incubated in basic medium for 3 hours at 37 °C before cell seeding. Cells were seeded on scaffolds with a density of 5000 cells/cm^2. Cells were cultured for 5 days with the medium being replaced every 2 days.

Cell penetration analysis: Samples were fixed with formalin for 30 min and then washed with PBS. To obtain cross-sections, the samples were cut half and embedded with Cryomatrix™ mounting media on mounting blocks with the cross-section facing upwards and then cut into 8 μm slices using a cryotome (Shandon Cryotome, Thermo Scientific). To avoid polymer auto-fluorescence, the cross-sections were stained with 1% (w/v) Sudan Black solution in 70% ethanol, incubated for 1 hour at room temperature, washed thoroughly with PBS for 5 × 5 min each. To visualize cell penetration into the scaffolds, their cross-sections were stained with DAPI. Briefly, samples were incubated with 1% Triton X-100 for 10 min on ice, washed with PBS, and blocked with bovine serum albumin (10 mg/mL) for 60 min to block unspecific binding. After removal of this solution, a DAPI solution (1:100 in PBS) was added for 15 min at room temperature avoiding light. Finally, all samples were washed with PBS and kept at 4 °C in the dark. Images were then taken using a fluorescent microscope (Nikon Eclipse E600).

To measure the penetration depth of cells in cross-sections, the fluorescent images were analyzed using Image J. Therefore, for each image, first the borders of the cross-section were defined and then a grid created dividing the depth or height of the section in 5 equally sized bins (Figure S9, Supporting Information), corresponding to depth ranges or regions from the top to the bottom of the scaffold. The first and last bin was considered the scaffold top and bottom, respectively. To normalize the data, the number of cells in each bin was divided by the total

amount of cells in the corresponding cross-section, and the infiltration depth ranges were divided by the scaffold thickness.

MLEC culture and seeding: MLEC, a kind gift from Dr. Daniel Rifkin from the Department of Cell Biology at the New York University School of Medicine, were stably transfected with an expression construct containing a truncated plasminogen activator inhibitor-1 (PAI-1) promoter fused to the firefly luciferase reporter gene. These cells are highly sensitive and specific for TGF-β production based on its ability to induce PAI-1 expression. MLEC were thawed and expanded in T-flasks till reaching 80% confluence in Dulbecco's Modified Eagle's Medium α (DMEM-α) supplemented with 10% FBS, 0.2 mM L-glutamine, and 100 units/mL penicillin and 100 mg/mL streptomycin. Samples were punched to fit a 96-well plate. After sterilization with 70% ethanol for 3×15 min each, the scaffolds were incubated in the described medium (without TGF-β1) overnight. The next day, the cells were seeded with a density of 50,000 cells/cm^2 on the scaffolds and on tissue culture plates used as a control. The cells were cultured for 5 days.

Luciferase and DNA assay: After removing medium, samples were washed thoroughly with PBS, and lysis buffer was added and diluted (5:1) in Milli-Q water. The samples were stored at -80 °C for at least 1 hour, and then defrosted on a plate shaker at room temperature. Each sample was divided, one half for the Luciferase and the other half for the DNA assay and transferred into a white and a black 96-well plate, respectively. For the Luciferase assay, Luciferase Assay Substrate (Promega) was added to the samples and the light produced was read on a plate reader (VICTOR 3, PerkinElmer) column by column.

DNA assay was performed using CyQUANT cell proliferation assay kit (Molecular Probes, Eugene, USA) according to the manufacturer's manual. Briefly, samples were supplemented with lysis buffer containing RNAse (Sigma) and incubated for 1 hour on a plate shaker, meanwhile a standard curve was prepared using λ DNA standard (provided from the CyQUANT kit). After the incubation period, CyQUANT GR dye in lysis buffer was added to the samples and the fluorescence was measured on a plate reader (VICTOR 3) at an excitation wavelength of 480 nm and an emission wavelength of 520 nm.

Statistical analysis: Statistical differences were determined using GraphPad Prism 5.001 software (San Diego, USA). Statistical differences between groups were determined using analysis of variance (ANOVA) followed by a Tukey's post-hoc test. Values are presented as mean ± standard deviation.

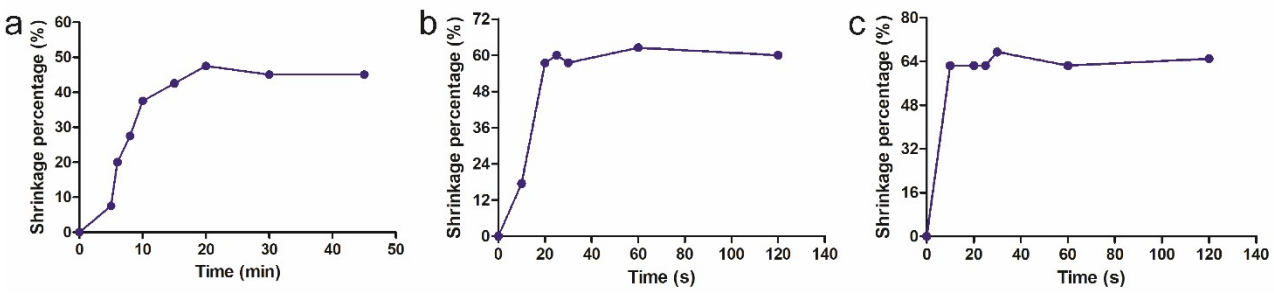

Figure S1. Shrinkage percentage of a monoaxially oriented PLA film as a function of heating time under different temperatures. (a) 65 ºC. (b) 75 ºC. (c) 85 ºC.

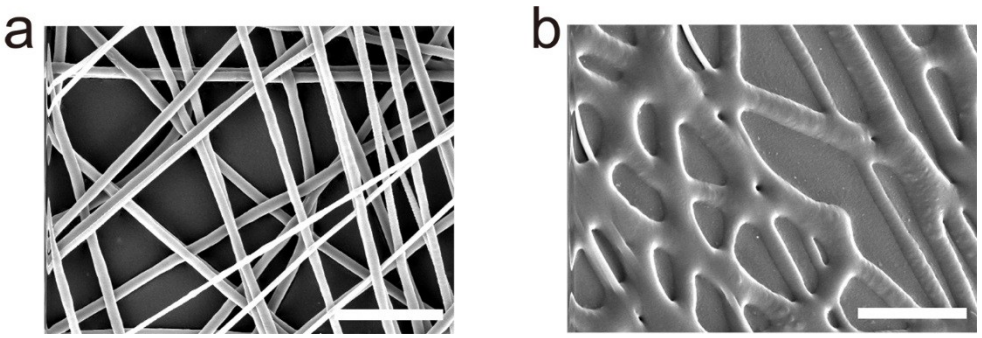

Figure S2. Failed buckling of PCL fibers on oriented PLA films. (a) PCL fibers before shrinking. (b) PCL fibers after shrinking. PCL fibers became molten and no crimped pattern could be observed. This was because the melting point of PCL is lower than the shrinking temperature of PLA. Scale bar: 20 μm.

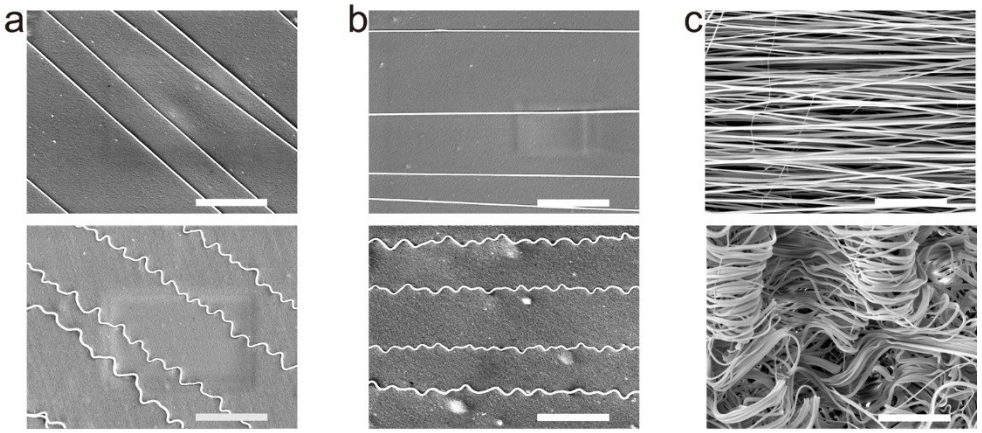

Figure S3. Fabricating curled PVA fibers using oriented PLA films. (a) Single fibers with alignment diagonal to the shrinking direction of the PLA film before (top) and after (bottom) shrinking. (b) Fibers with alignment parallel to the shrinking direction of the PLA film before (top) and after (bottom) shrinking. (c) Fiber mesh with alignment parallel to the shrinking direction of the PLA film before (top) and after (bottom) shrinking. Scale bar: 20 μm.

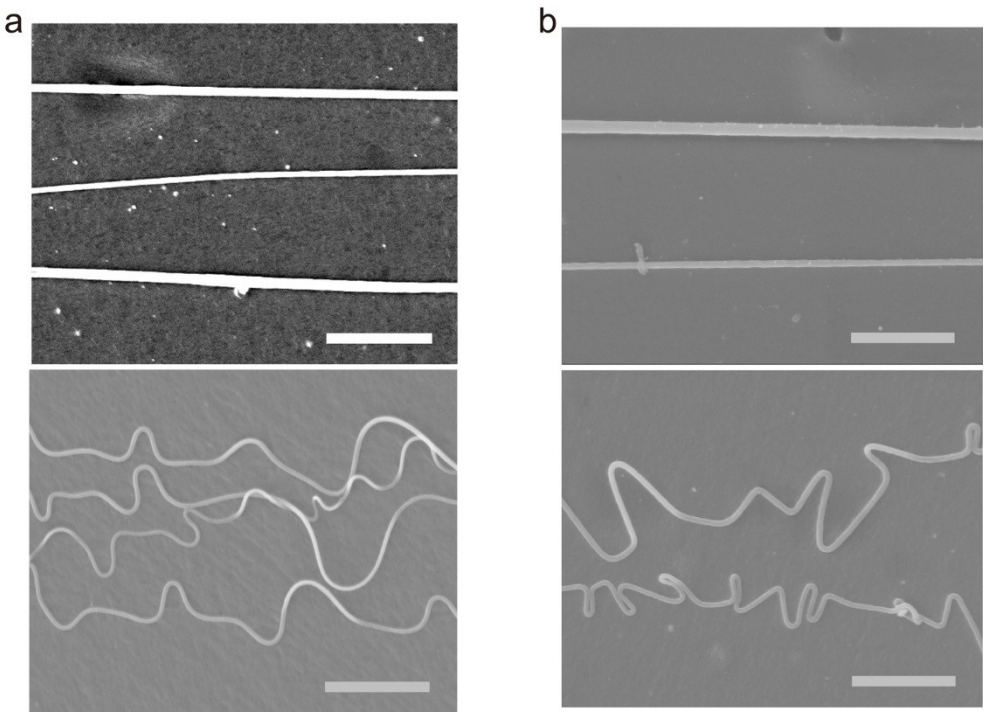

Figure S4. Fabrication of PAN and PS fibers using oriented PLA films. (a) PAN fibers deposited on PLA films before (top) and after (bottom) shrinking. (b) PS fibers deposited on PLA films before (top) and after (bottom) shrinking. Scale bar: 10 μm.

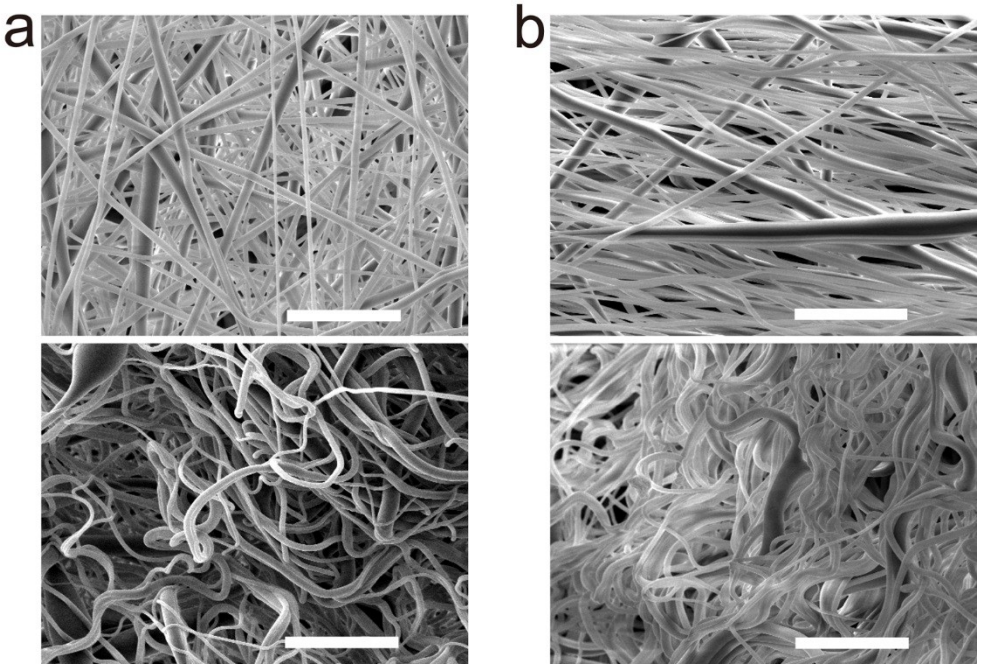

Figure S5. Fabricating curled PEOT/PBT fibers using oriented PS films. (a) Random PEOT/PBT fibers deposited on PS films before (top) and after (bottom) shrinking. (b) Aligned PEOT/PBT fibers deposited on PS films before (top) and after (bottom) shrinking. Scale bar: 20 μm.

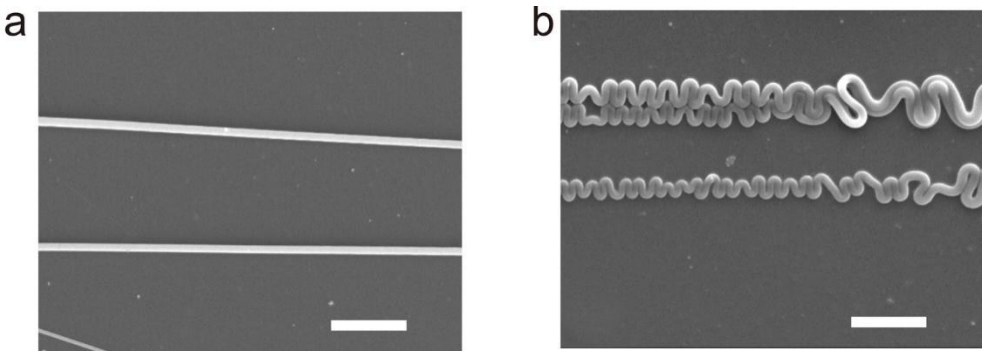

Figure S6. Fabricating curled PAN fibers using oriented PS films. (a) PAN fibers deposited on PS films before shrinking. (b) PAN fibers deposited on PS films after shrinking. Scale bar: 10 μm.

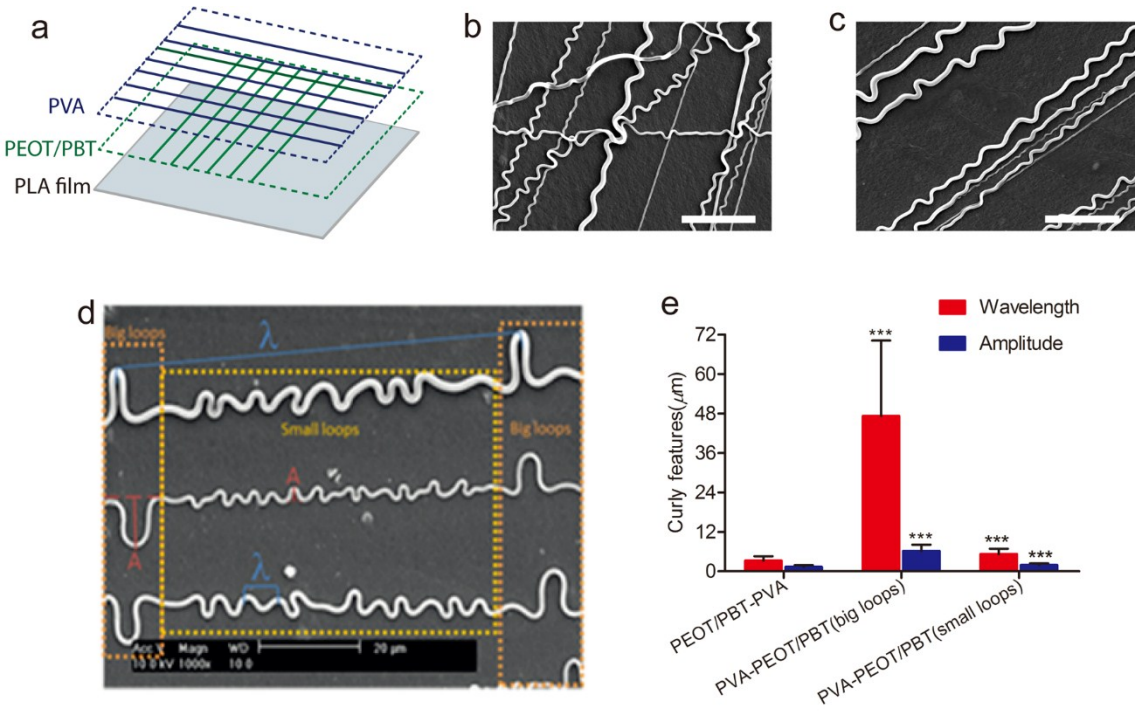

Figure S7. Adjusting curled patterns via introducing a sacrificial fiber layer. (a) Illustration of fabricating PEOT/PBT-PVA fibers. PEOT/PBT fibers were first deposited on the surface of the PLA film, then a second layer of PVA fibers was deposited on top of it. (b) SEM image of curled PEOT/PBT-PVA fibers before sacrificing the PVA fibers. (c) Morphology of curled PEOT/PBT-PVA fibers after sacrificing the PVA fibers. Fibers only have curls of similar size while curled PVA-PEOT/PBT fibers after scarifying PVA fibers present curls of two different sizes (big loops and small loops). (d) Figure depicting the ways to measure wavelengths and amplitudes for big loops and small loops observed in PVA-PEOT/PBT fibers after scarifying PVA fibers. (e) Comparison of curly features (wavelengths and amplitudes) between PEOT/PBT-PVA and PVA-PEOT/PBT fibers after scarifying PVA fibers. PEOT/PBT-PVA corresponds to PEOT/PBT as first layer of deposition and PVA as second layer, and PVA-PEOT/PBT corresponds to PVA as first layer and PEOT/PBT as second layer. The distinction between big loops and small loops is explained in (d), where the same fiber has curls of two different sizes that were measured separately. ***$p < 0.001$, comparison with PEOT/PBT-PVA. Scale bar: 20 μm (b and c).

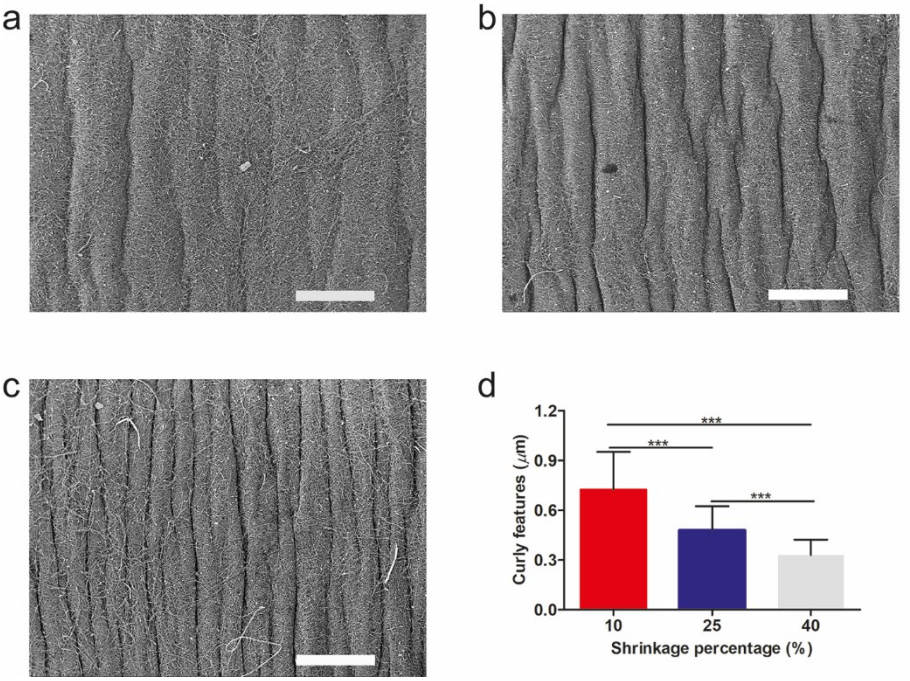

Figure S8. Influence of shrinkage percentage on wavy feature. (a) Morphology of wavy pattern at 10% shrinkage percentage. (b) Morphology of wavy pattern at 25% shrinkage percentage. (c) Morphology of wavy pattern at 40% shrinkage percentage. (d) Quantification of curly features generated from different shrinkage percentage. ***$p < 0.001$. Scale bar: 1 mm.

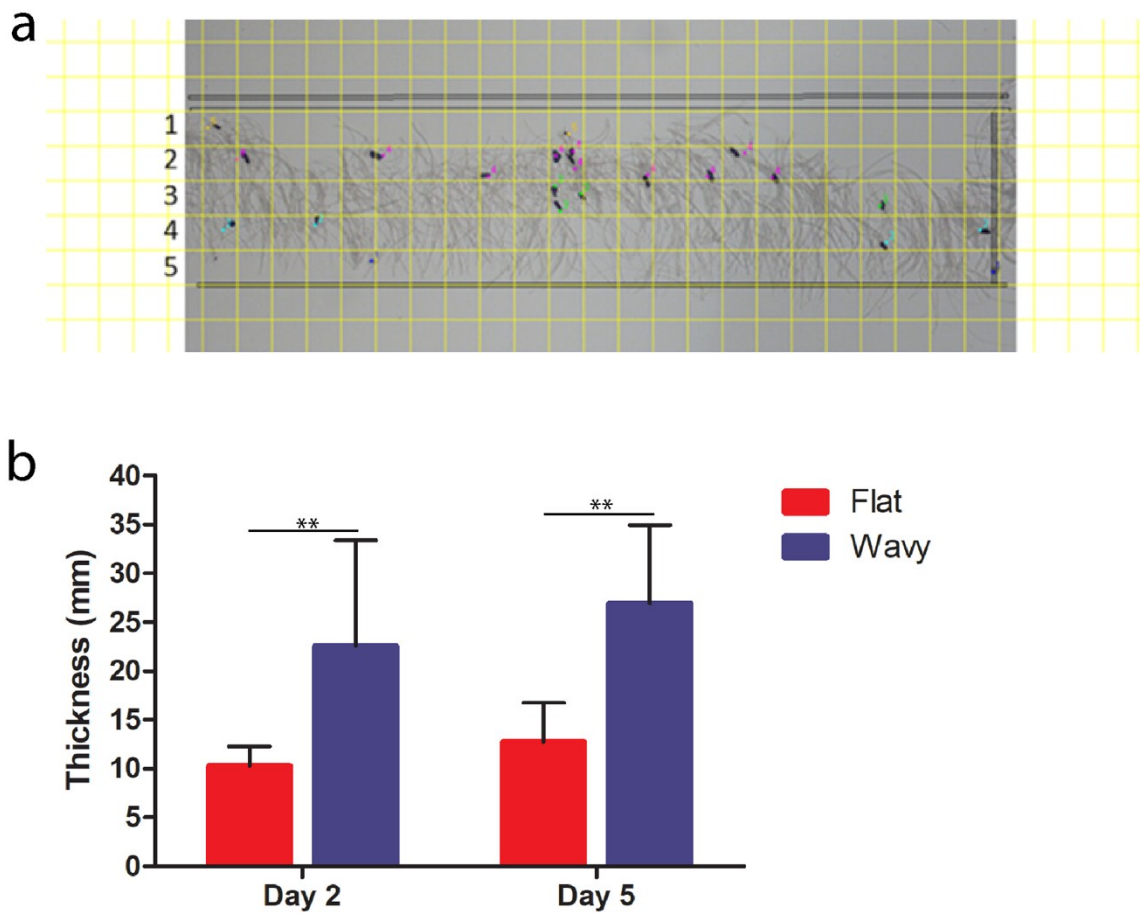

Figure S9. Quantification of cells infiltration into scaffolds (a) Grid created in ImageJ to measure cell infiltration along the cross-section. The numbers represent the bins for each scaffold cross-section, 1 corresponding to the top and 5 to the bottom; (b) Graph showing the doubling effect in thickness observed after shrinkage. **$p < 0.05$.

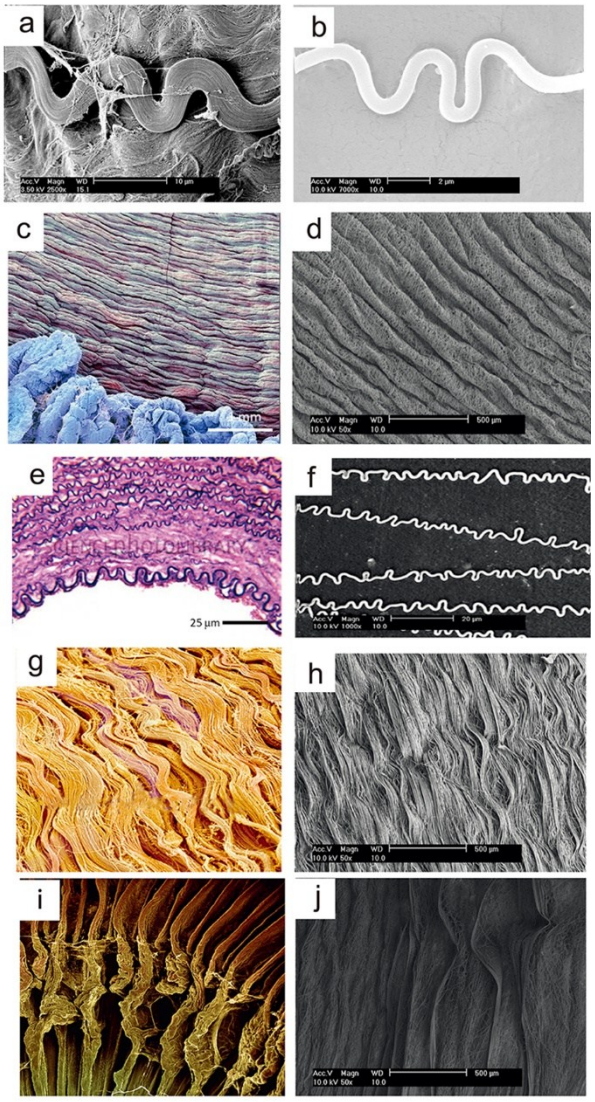

Figure S10. Similarities between native tissues and obtained fibers or meshes. (a) SEM image of musculoskeletal tissue composed wavy fibers. (b) Fibers fabricated in the present study exhibiting a similar wavy configuration to (a). (c) SEM image of the human iris (scale bar: 1 mm; from www.sciencephoto.com). (d) Features of the scaffold in the present study showing a similarity to that of the iris in (c). (e) Image of a human artery wall composed of curled elastin bundles separated by collagen (from www.sciencephoto.com). (f) Shrunk low-density scaffold from the present study resembling the structure in (e). (g) SEM image of a tracheal wall displaying a crimp pattern (from www.sciencephoto.com). (h) High-density shrunk scaffold from the present study resembling (g). (i) SEM image of a ciliary body (from https://fineartamerica.com). (j) Structure obtained in the present study having similarity to (i).

Table S1. Mechanical analysis.

Shrinkage (%)	Young's modulus (MPa)	Linearity range (%)	Ultimate stress (MPa)	Ultimate strain (%)	Strain energy density (MPa)
0	9.91 ± 2.24	1-7	2.75 ± 0.76	131.78 ± 29.42	3.04 ± 0.87
10	5.12 ± 1.15	1.8-10	2.24 ± 0.33	245.96 ± 21.37	4.66 ± 0.77
25	6.49 ± 1.64	1.8-10	2.69 ± 0.47	199.18 ± 37.93	5.28 ± 1.67
30	4.61 ± 1.16	1-7	1.24 ± 0.20	112.64 ± 37.74	1.27 ± 0.50
40	2.87 ± 0.46	1-9	1.37 ± 0.32	150 ± 32.56	1.76 ± 0.53
50	2.40 ± 0.31	1-12	1.13 ± 0.15	124.9 ± 26.64	1.19 ± 0.25

Supplementary note: Mechanical modelling

The results of the model fitting are summarized in Table S2.

Table S2. Mooney-Rivlin model: parameter estimation.

Shrinkage percentage (%)	C01	C10	C20	R^2
0	3.39 ± 1.33	-1.43 ± 0.89	0.130 ± 0.120	0.962 ± 0.011
10	1.29 ± 0.24	-0.17 ± 0.08	0.007 ± 0.003	0.974 ± 0.007
25	2.06 ± 0.54	-0.47 ± 0.25	0.022 ± 0.011	0.972 ± 0.003
30	1.93 ± 0.79	-0.91 ± 0.57	0.081 ± 0.062	0.986 ± 0.003
40	1.28 ± 0.41	-0.44 ± 0.27	0.032 ± 0.024	0.961 ± 0.011
50	1.13 ± 0.50	-0.37 ± 0.34	0.032 ± 0.041	0.982 ± 0.018

A statistically significant decrease of the parameter C_{01} with the increase of the shrink percentage was detected. A similar trend was found for the parameter C_{10}. No statistical differences were found among the different percentages of shrinkage for the parameter C_{20}.

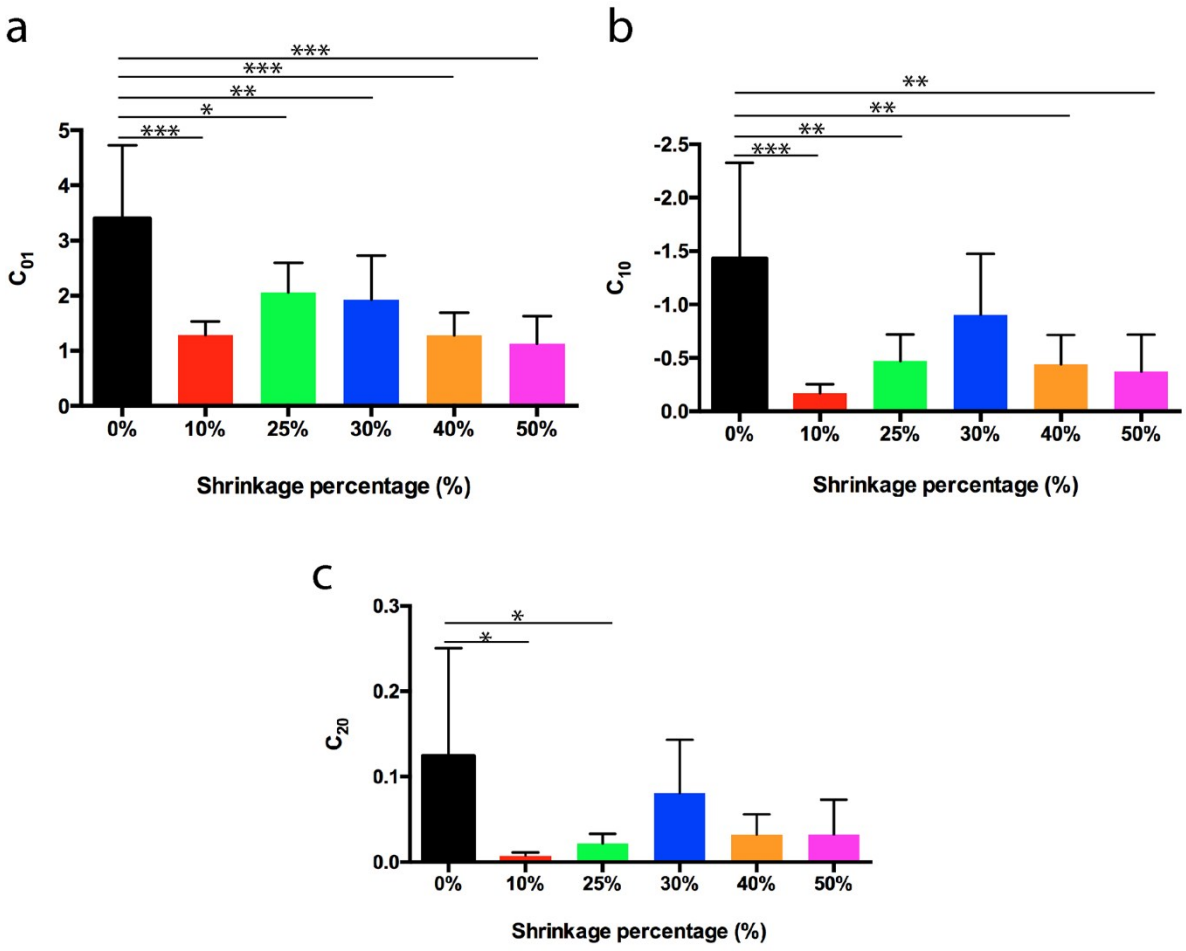

Figure S11. Mooney-Rivlin model: comparisons of different conditions for each parameter. (a) Parameter C_{01}. (b) Parameter C_{10}. (c) Parameter C_{20}.